Supplementary Material for Self-diffusion in Ferrogranulates: Stockmayer Model Revisited

Oksana Bilous[a], Kirill A. Okrugin[a], Ali Lakkis[b], Reinhard Richter[b], Sofia Kantorovich[a]

[a]*University of Vienna, Faculty of Physics, Kolingasse 14-16, Vienna, Austria*
[b]*University of Bayreuth, Experimental Physics, Universitätsstrasse 30, Bayreuth, Germany*

Here we provide an additional information on magnetic particle clustering and self-diffusion.

1. Cluster Analysis

In Table S1, we collected the actual values of the area fractions of clustered, single, and migrating magnetic particles, shown in Fig. 2 of the main manuscript. At B_0^*, the fraction of clustered particles dominates, with minimal contributions from single and migrating particles. At B_1^*, the fraction of clustered particles decreases, while that of migrating particles increases. At B_2^*, the fraction of clustered particles decreases further, and the fractions of both single and migrating particles increase, indicating the breakage of clusters.

Table S1: The area fractions of the magnetic particles in clusters (ϕ_{clus}), of single ones (ϕ_{sing}), and of migrating ones (ϕ_{migr}) as a function of the applied external magnetic induction B^*.

	$B_0^* = 0.0$	$B_1^* = 0.5$	$B_2^* = 1.0$
ϕ_n	$\phi_{\text{clus}}/\phi_{\text{sing}}/\phi_{\text{migr}}$	$\phi_{\text{clus}}/\phi_{\text{sing}}/\phi_{\text{migr}}$	$\phi_{\text{clus}}/\phi_{\text{sing}}/\phi_{\text{migr}}$
ϕ_1	0.090/0.006/0.004	0.070/0.020/0.010	0.010/0.070/0.020
ϕ_2	0.100/0.006/0.014	0.080/0.020/0.020	0.020/0.060/0.040
ϕ_3	0.120/0.006/0.007	0.100/0.020/0.013	0.030/0.060/0.043
ϕ_4	0.140/0.006/0.007	0.110/0.020/0.023	0.050/0.050/0.053
ϕ_5	0.150/0.007/0.013	0.130/0.020/0.020	0.070/0.050/0.050
ϕ_6	0.160/0.007/0.006	0.130/0.020/0.023	0.070/0.050/0.053
ϕ_7	0.160/0.007/0.013	0.140/0.010/0.030	0.080/0.050/0.050
ϕ_8	0.180/0.005/0.015	0.120/0.020/0.060	0.090/0.050/0.060

2. Self-Diffusion

The separation between different particle categories used in this work can be further appreciated by looking at representative one-particle trajectories (often referred to in the literature as single-particle trajectories or SPTs [1–3]; however, here they should not be confused with non-aggregated particles). Fig. S1 presents typical simulation trajectories for single Stockmayer particles (a); Stockmayer particles in a cluster; (c) migrating Stockmayer beads; and (d) purely repulsive beads at $\phi_8 = 0.350$ and

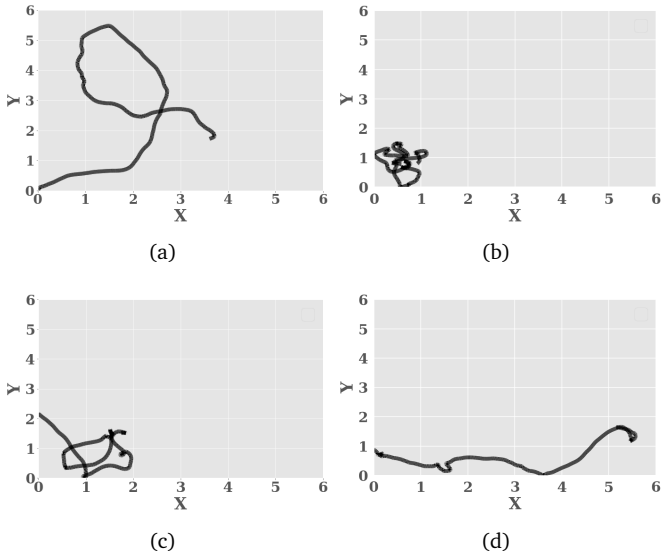

Figure S1: Individual trajectories obtained in simulations: (a) single magnetic particle; (b) magnetic particle within cluster; (c) migrating magnetic particle; (d) glass particle for the constant highest area fractions $\phi_8 = 0.350$ in the absence of induction, $B_0^* = 0$. The trajectories are shifted to ease the comparison.

$B_0^* = 0$. As mentioned in the main article, the time window is selected to be 2×10^4 integration steps. While the behaviour of a single magnetic or nonmagnetic particle (compare (a) to (d)) is as expected, corresponding to a random-walk-like motion, the trajectory of a particle in a cluster is very constrained and clearly non-uniform. As commented in the main manuscript, this results not only in subdiffusive behaviour but also in a peculiar non-Gaussianity of the particle displacement distributions, depending on the cluster size and morphology.

In Fig. S2, we present typical mean-square displacement (MSD) curves.

Fig. S2 also compares the MSD of glass beads and magnetic particles bound in clusters for two representative area fractions in the absence of magnetic induction. In both cases, glass beads display nearly ballistic scaling, whereas clustered magnetic particles exhibit a markedly reduced exponent, reflecting their constrained motion. The vertical markers indicate the lag times τ_i at

Email address: oksana.bilous@univie.ac.at (Sofia Kantorovich)

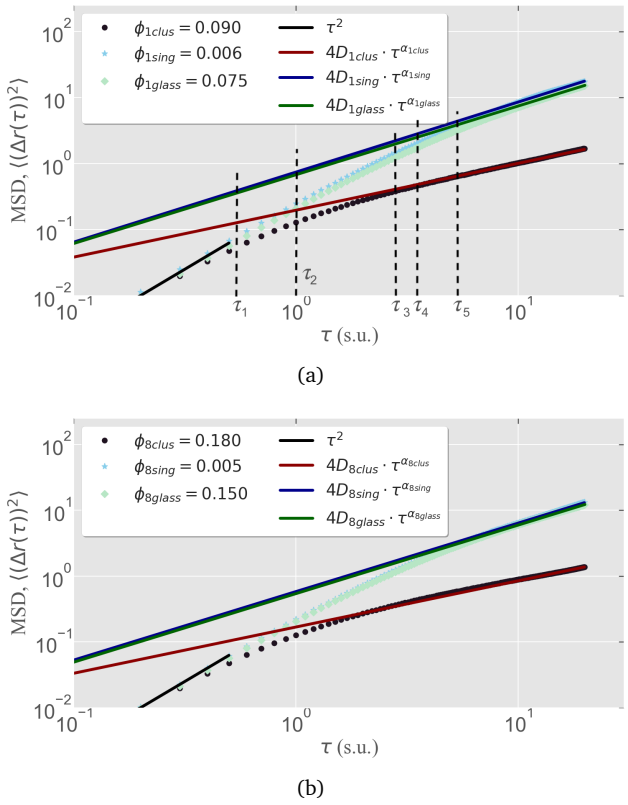

Figure S2: Computed mean square displacement (MSD) as a function of the lag time for glass beads (dots) and magnetic particles within clusters (black circles) at two total area fractions: (a) $\phi_1 = 0.175$ and (b) $\phi_8 = 0.350$. No magnetic induction was applied ($B_0^* = 0$). The dotted black line shows a quadratic fit, and the coloured lines indicate the diffusion equation (7) (main text) for single, glassy, and clustered particles. Vertical dashed lines mark the lag times τ_i used for displacement analyses.

which displacement distributions (shown below) and non-Gaussianity parameters are evaluated (in the main text).

3. Displacement Distributions

The raw displacement distributions shown in Fig. S3 illustrate the statistics underlying the non-Gaussian parameter γ_2 for single (non-aggregated) magnetic particles. Panels (a), (c), and (e) correspond to B_0^* at area fractions ϕ_1, ϕ_4, and ϕ_8, respectively, while panels (b), (d), and (f) show the corresponding results for B_2^*. Each curve represents the frequency of particle displacements at a given lag time τ_i, obtained by averaging over eight independent simulation runs. The vertical axes display the raw counts on a logarithmic scale, allowing the statistical quality of the data to be directly assessed. In the absence of an applied induction, the distributions remain close to Gaussian across all τ_i, with deviations becoming noticeable only at the highest area fraction. Under strong induction, the distributions broaden significantly and develop extended non-Gaussian tails, reflecting the enhanced dynamical heterogeneity caused by dipolar repulsion between field-aligned single particles.

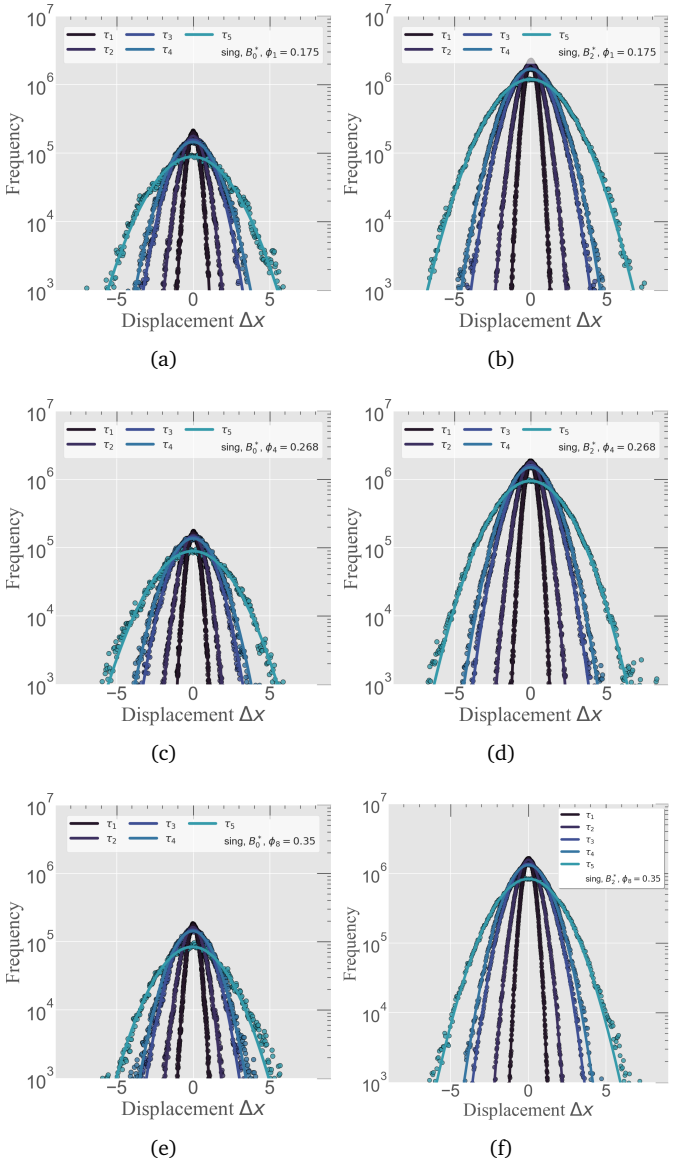

Figure S3: Raw displacement frequencies for single (non-aggregated) magnetic particles at various lag times τ_i. Panels (a), (c), and (e) show the results in the absence of an applied induction, B_0^*, for increasing area fractions ϕ_1, ϕ_4, and ϕ_8, respectively. Panels (b), (d), and (f) present the corresponding data under strong induction, B_2^*.

The raw displacement distributions presented in Fig. S4 show the underlying statistics for particles that belong to clusters. Panels (a), (c), and (e) again correspond to B_0^* at area fractions ϕ_1, ϕ_4, and ϕ_8, respectively, while panels (b), (d), and (f) display the corresponding results for B_2^*.

In contrast to single non-aggregated particles, the distributions for clustered particles exhibit strongly non-Gaussian shapes even at B_0^*, with broad, heavy tails that reflect the heterogeneous and constrained dynamics inside aggregates. At B_2^*, the distributions become even more pronouncedly non-Gaussian, particularly at intermediate and long lag times, where field-induced restructuring leads to compact clusters and intermittent, spatially restricted motion.

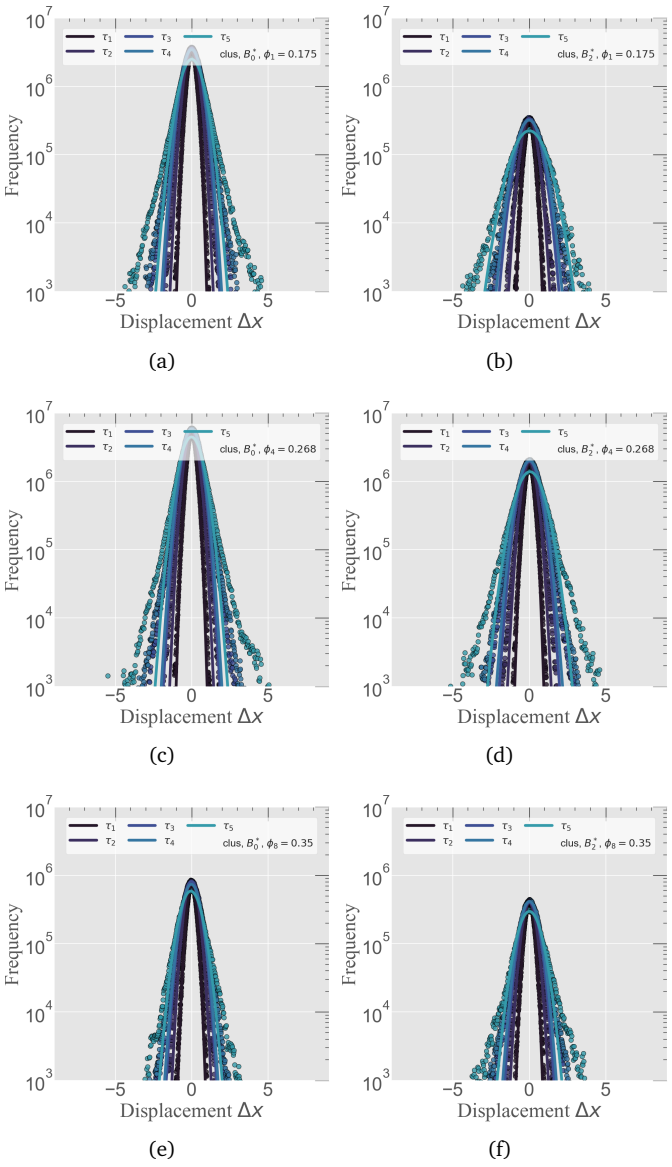

Figure S4: Raw displacement frequencies for single (non-aggregated) magnetic particles at various lag times τ_i. Panels (a), (c), and (e) show the results in the absence of an applied induction, B_0^*, for increasing area fractions ϕ_1, ϕ_4, and ϕ_8, respectively. Panels (b), (d), and (f) present the corresponding data under strong induction, B_2^*.

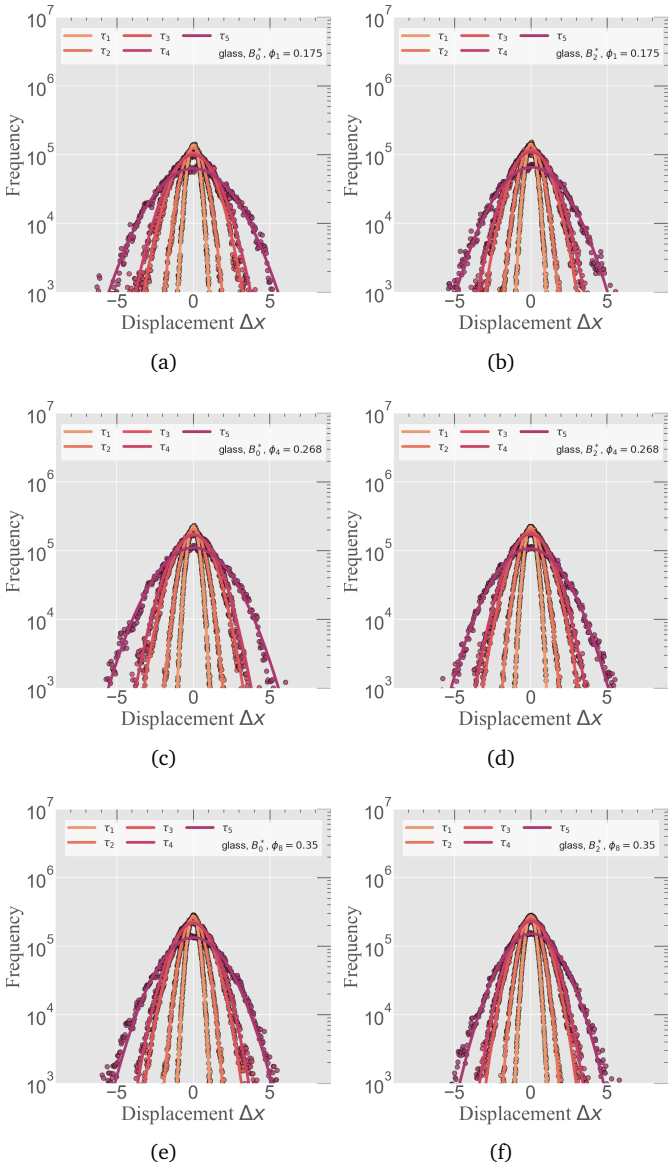

Figure S5: Raw displacement frequencies for magnetic particles in clusters at various lag times τ_i. Panels (a), (c), and (e) show results for B_0^* at ϕ_1, ϕ_4, and ϕ_8, while (b), (d), and (f) present the corresponding data for B_2^*.

Fig. S5 follows the same naming convention as the previous two figures and shows the frequencies of displacements for glass particles. Here, similarly to single magnetic particles, at B_0^*, the distributions are Gaussian; however, they clearly broaden at B_2^*, particularly for high values of ϕ_n and τ_i.

References

[1] A. Kusumi, T. A. Tsunoyama, K. M. Hirosawa, R. S. Kasai, T. K. Fujiwara, Paradigm shift of the plasma membrane concept from the two-dimensional continuum fluid to the partitioned fluid: High-speed single-molecule tracking of membrane molecules, Annu. Rev. Biophys. Biomol. Struct. 34 (2005) 351–378. doi:10.1146/annurev.biophys.34.040204.144637.

[2] D. Ernst, J. Köhler, M. Weiss, Probing the type of anomalous diffusion with single-particle tracking, Phys. Chem. Chem. Phys. 16 (2014) 7686–7691. doi:10.1039/C4CP00292J.

[3] F. Simon, L. E. Weiss, S. van Teeffelen, A guide to single-particle tracking, Nature Reviews Methods Primers 4 (2024) 66. doi:https://doi.org/10.1038/s43586-024-00341-3.